This document was prepared in conjunction with work accomplished under Contract No. DE-AC09-96SR18500 with the U. S. Department of Energy.

DISCLAIMER

WSRC-MS-2006-00161

Erosion Evaluation of a Slurry Mixer Tank with Computational Fluid Dynamics Methods

by

SI LEE

Westinghouse Savannah River Company
Savannah River Site
Aiken, South Carolina 29808

Additional Authors:
RICHARD DIMENNA
GLENN TAYLOR

DOE Contract No. **DE-AC09-96SR18500**

Proceedings of ICONE 14
International Conference on Nuclear Engineering
July 17-20, 2006, Miami, Florida, USA
ICONE14-89309

Erosion Evaluations of a Slurry Mixer Tank with Computational Fluid Dynamics Methods

Si Y. Lee*, Richard A. Dimenna, and Glenn A. Taylor
Savannah River National Laboratory
Washington Savannah River Company
Aiken, SC 29808
si.lee@srnl.doe.gov, richard.dimenna@srnl.doe.gov, glenn.taylor@srl.doe.gov
*803-725-8462

ABSTRACT

This paper discusses the use of computational fluid dynamics (CFD) methods to understand and characterize erosion of the floor and internal structures in the slurry mixing vessels in the Defense Waste Processing Facility. An initial literature survey helped identify the principal drivers of erosion for a solids laden fluid: the solids content of the working fluid, the regions of recirculation and particle impact with the walls, and the regions of high wall shear.

A series of CFD analyses was performed to characterize slurry-flow profiles, wall shear, and particle impingement distributions in key components such as coil restraints and the vessel floor. The calculations showed that the primary locations of high erosion resulting from abrasion were at the leading edge of the coil guide, the tank floor below the insert plate of the coil guide support, and the upstream lead-in plate. These modeling results based on the calculated high shear regions were in excellent agreement with the observed erosion sites in both location and the degree of erosion. Loss of the leading edge of the coil guide due to the erosion damage during the slurry mixing operation did not affect the erosion patterns on the tank floor. Calculations for a lower impeller speed showed similar erosion patterns but significantly reduced wall shear stresses.

Keywords: Erosion Evaluations, Slurry Mixer Tank, Computational Fluid Dynamics Model

INTRODUCTION AND BACKGROUND

A visual inspection of the Slurry Mixer Evaporator (SME) tank interior done recently at the Savannah River Site (SRS) Defense Waste Processing Facility (DWPF) revealed areas of significant erosion on the tank floor in the vicinity of the cooling coil guides, as well as the erosion and in some cases complete absence of portions of internal structures. This erosion of the high-level waste mixer tank has been investigated in an attempt to identify the root cause so that corrective actions could be taken before the tank integrity was compromised. Figure 1 is a sketch of the tank and model geometry including the cooling coil guide pins and geometrical shapes of the guide structure.

The erosion in the SME occurred in localized areas around the coil guides. There are four coil guides located in the bottom of the tank as shown in Fig. 1. Each coil guide has similar erosion characteristics. A recent inspection conducted by DWPF Engineering identified severe erosion to the leading edge of the guide, scouring of the base metal, and loss of the top lead-in plate. The guides protrude into the flow stream and can cause a vortex that can tend to scour the exposed surfaces of the guides. This generates secondary flow circulation and results in waste fluid staying in contact with the downstream horizontal surface below the coil support insert (see Fig. 1). When the solids-laden slurry comes in contact with the wall surface, it can remove wall material through the process of erosion. It was postulated that the mechanical interactions of the ambient fluid and solids against the wall surface leading to erosion could be identified by the wall shear, the tangential force per unit area applied by the moving fluid on the bounding wall.

A literature survey was performed previously to identify the principal mechanisms of wear for a solids laden fluid and to find out what other wear studies and experiments have been done. Available evidence suggests that the key to understanding erosion in flow systems is a detailed knowledge of the coupled and complex phenomena of solids circulation and fluid motion. Wear on the tank wall, or erosion, occurs from the coupled behavior of the abrasive solids in the slurry and the wall shear of viscous liquid. Chemicals in the slurry may also result in corrosion and can lead to a synergistic effect of both erosion and corrosion. In this work, the erosion mechanism without any chemical reactions is considered as the primary cause of wear. This assumption, which serves to simplify the problem, is justified by a material study done on the damaged tank surface which concluded that corrosion was unlikely [1].

This paper presents the application of computational fluid dynamics (CFD) methods to a qualitative estimate of the erosion phenomena expected in the SME and a sister tank, the Melter

Feed Tank (MFT), by calculating erosion drivers. Using the transport equations governing the slurry flow, two erosion mechanisms were considered to evaluate high erosion sites and investigate the primary cause of erosion damage. One of the two mechanisms is abrasive erosion caused by high wall shear of the viscous liquid or by continuous contact or low-angle collisions of the moving solids with the rough surface. The other is the chip-off erosion which is driven by high-angle impingement of particles on the surface. Ductile wall material such as stainless steel is damaged by the wall shear mechanism when particles contact the ductile surface without separating from an accelerated fluid characteristic of a closed- or curved- flow path. Previous results [2] showed that the primary locations of high erosion due to particle impingement occurred in regions of sudden changes in flow direction, contractions, and flow obstructions.

A key concern with radioactive operation of a piping system is the integrity of the tank, cooling coil fittings, and accompanying equipment. A breach could release contamination, which at a minimum would increase operational costs due to clean up and down time, but more importantly, would increase the potential radiation exposure to personnel. It is very important to thoroughly understand the effects of erosion caused by slurry flow so that proper maintenance can minimize equipment failure and guarantee safe operation.

The primary objective of the work is to identify potential locations of high erosion for the SME/MFT coil guides and its support structures as shown in Fig. 1. The SME and MFT are similar process vessels with nearly identical geometry. Both vessels have coil banks and identical agitators, but they don't have any baffles. The agitator is located at the center of the tank and has two impellers as shown in figure. The upper blade is a propeller to circulate fluid in the axial direction. The lower blade is a Rushton-type flat-blade impeller. This type of impeller directs flow in the radial direction. The SME agitator operates at 130 and 65 rpm, whereas the MFT agitator operates at 103 and 65 rpm. The coil banks, while not solid, provide a sufficiently strong cross-flow resistance that they effectively isolate the inner third of the tank from the outer two-thirds and restrict the discharge from the impellers to the bottom of the tank.

NOMENCLATURE

Conc. = concentrations
DWPF = Defense Waste Processing Facility
cp = centipoise
=0.001 Pa-sec
g = acceleration due to gravity (m/sec^2)
Pa = (N/m^2)
Re = Reynolds number ($d\rho u/\mu$)
d = diameter
NDE = Non-destructive examination
MFT = melter feed tank
rpm = revolutions/min
sg = specific gravity
SME = slurry mixer evaporator
SRS = Savannah River Site
θ = incident angle

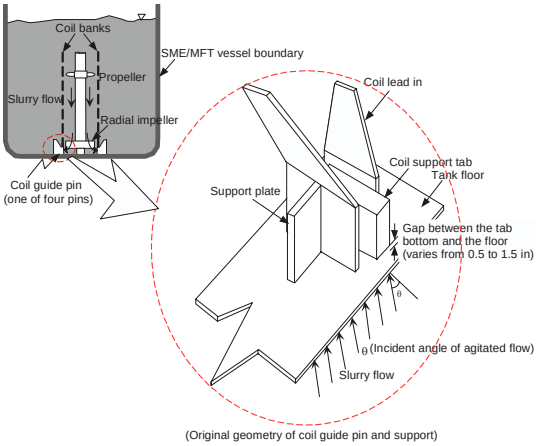

Figure 1. Modeling geometry considered for the present analysis

EROSION OBSERVATIONS AND MEASUREMENTS OF SLURRY MIXER EVAPORATOR VESSEL

Non-Destructive Examination (NDE) with ultrasonic testing was used to evaluate the wall thickness and general condition of the SME tank bottom. The lower coil ring has four coil tabs used for alignment and stability. Each coil tab sets into the middle of a coil guide attached to the tank bottom. The coil bank is suspended from the top of the tank, so it is level. The tank bottom, on the other hand, is inclined, so there are different gap sizes between the lower end of the coil tab and the tank floor ranging from 0.5 inch in Zone C to 1.5 inches in Zone A. This configuration is shown in Fig. 2. Nominal wall thickness of the SME tank bottom is approximately 0.75 inches. Areas of specific interest were the areas surrounding the four coil guides and the circumferential area under the lower coil ring. The test results showed significant wall erosion occurred at the areas near the base of the coil guides. A minimum wall thickness of 0.4 inches under the coil tab with the smallest gap of 0.5 inches was observed by the NDE technique, implying a 0.35-in deep cavity on the floor of the mixing vessel as shown in Fig. 2.

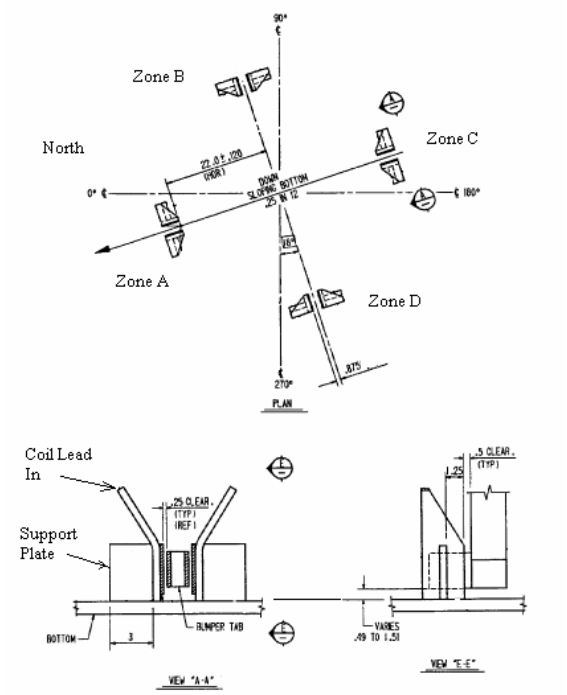

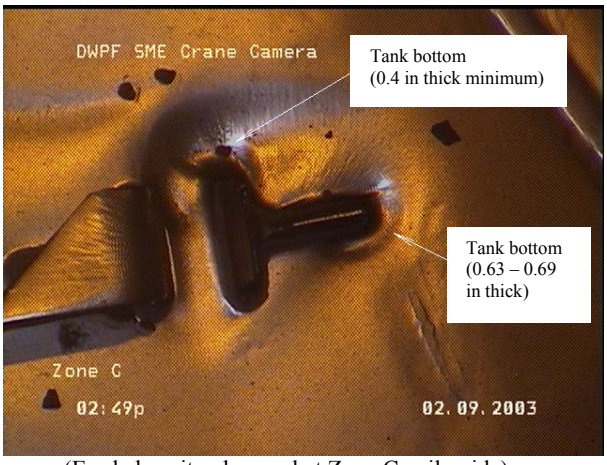

(Eroded cavity observed at Zone C coil guide)

Figure 2. Four coil guides and observed surface erosion near one of the four guides on the floor of Slurry Mixer Evaporator Vessel.

COMPUTATIONAL MODELS

Figure 1 shows the modeling and computational domains used for the present analysis including the original guide pin geometry in the SME tank. The computational domain was deliberately kept small to minimize the size of the numerical model and the associated computational time. Nonetheless, upstream flow information was included from the global model to ensure the flow pattern reaching the domain boundary of the SME guide pin would be close to that actually occurring in the tank. Because of the close proximity of the coil guides to the discharge of the radial impeller and the tendency of the cooling coils to isolate the impeller inlet flow from the outer annulus of the tank, the inlet flow to the guide pin model is not affected by the flow past the guide pin. Therefore, a global model was developed to calculate a good approximation to the boundary flow for a local domain around the eroded area.

The modeling effort was performed in two stages for computational efficiency. First was the global model, which included the mechanical agitator and tank boundary as the computational domain to evaluate the upstream flow field of each coil guide and to estimate overall flow patterns near the boundary of the cooling coil guide. This was evaluated for the three different rotational speeds of the SME or MFT agitator. The flow field calculations were performed with the Fluent^{TM} code. The second stage was a detailed model to evaluate the flow field surrounding the coil guide. The boundary conditions for this model were based on the results provided from the first model.

This paper will focus on the results from the detailed model. The calculations performed here will be used to identify the potential locations of high erosion for the SME vessel, coil guide and its support structure, and to estimate the maximum allowable speed of the MFT agitator.

Two different modeling domains were used to examine how sensitive the flow and erosion patterns are to the geometrical change in the coil guide as shown in Fig 1. Based on the configurations shown in Fig. 1 and the operating conditions shown in Table 1, the erosion evaluations for two different cases were performed, one for the coil guides in their original configuration and a second with the upstream lead-in plate removed. The analyses were performed to provide information on erosion drivers for the areas near the four cooling coil guides and to examine how sensitive the flow patterns and high erosion locations are to the disappearance of the lead-in plate as result of the erosion process as shown in Table 2.

Erosion pattern calculations were performed for both postulated driving mechanisms: wall shear and particle impingement. Early in the analysis, it was observed that the wall shear patterns agreed well with observations in the tank, whereas the particle impingement patterns did not. Therefore, all subsequent work assumed that material erosion was governed primarily by the wall shear mechanism wherein particles are homogeneously distributed in the slurry flow and the impingement angles of the particles against the wall surface are small. In light of this observation, the wall shear model will be used to provide qualitative information on flow patterns and potential erosion damage locations.

For the calculations of the continuous slurry flow field, three-dimensional transport and continuity equations were solved in an Eulerian reference system. Detailed governing equations for the continuous phase were provided in the previous work [2,3]. Reynolds number for the flow condition is found to be in the range of about 10^5 (based on tank

diameter), which corresponds to a fully turbulent regime. A two-equation turbulence model with turbulent kinetic energy and dissipation equations, the standard $\tilde{k}$-ε model, was used to include the effects of particle dispersion due to turbulent eddies in the continuous phase. The wall boundary region used standard wall function. All the detailed governing equations are not repeated here since they are provided in the previous work [3]. For the wall shear model, field solutions for the Eulerian equations of the continuous slurry flow were applied to estimate wall shear stress. To simulate particle impingement trajectory, a momentum balance, including inertia, solid-fluid interfacial drag, and gravitational terms, was used in a Lagrangian reference system to calculate the trajectory of the discontinuous particles in the slurry. Thus, a Lagrangian-formulated deterministic particle equation of motion was solved via an integral method to predict particle speeds and trajectories once the continuous flow field was known. All converged solutions for the governing equations were achieved using the segregated and iterative solution technique.

The analysis addresses flow patterns expected for the coil guide geometry, as well as the specific erosion mechanisms for a slurry flow, wall shear stress and particle impingement. Particle concentration of the mixed fluid is about 19 volume percent corresponding to 30 wt% particles. The solid particles in the SME slurry are principally glass frit, which are very abrasive. The average primary flow velocity is in the range of 0.65 to 1.8 m/sec as shown in Table 1. These velocities were derived from the flow field results of the global model.

The wall erosion of the mixing vessel under a homogeneous solid-fluid flow regime is caused mainly by abrasive wall friction, since the solids in the viscous fluid of about 10 cp do not separate readily from the bulk fluid motion. Ductile wall material such as Hastalloy or stainless steel is damaged by an abrasive mechanism when particles impinge on the surface with essentially wide-open space and no closed- and curved- flow path. Previous results [3] showed that the primary locations of high erosion due to particle impingement were at regions of a sudden change of flow direction, sudden contraction, or flow obstruction. For a slurry flow with solids content, the particle impingement process may not be important compared to the abrasive shear-driven erosion mechanism because the solid-fluid mixture flows like a homogeneous fluid due to the high interfacial drag. In addition, the coil guide geometry has a large open space without any sudden change of flow direction.

Table 1. Input parameters for the present calculations

Parameters		Input data
Bulk slurry specific gravity		1.35 sg
Slurry viscosity		10 cp
Slurry velocity at the model boundary (agitator speed)		0.65 m/sec (65 rpm), 1.8 m/sec (130 rpm), and 1.3 m/sec (103 rpm)
Solids in slurry flow	Average diameter	100 microns
	Density	2.43 gm/cc
	Solid fraction	30 wt%*

Note: *This corresponds to 19.2 vol.% solids in fluid.

Table 2. Modeling cases considered in the analysis

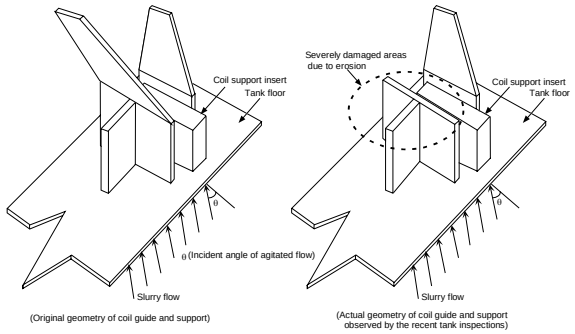

(Nominal model: Case-A) (Case-B)

Modeling cases	Modeling domain (shown above)	Primary objective
Case-A (Nominal model)	Original undamaged coil guide	To estimate flow patterns associated with abrasive erosion due to wall shear
Case-B	Actual damaged coil guide as observed in the flow domain	To examine sensitivity of flow patterns and erosion locations due to the loss of flow obstructions

Modeling assumptions made for the calculations:

- The present models consider only mechanical erosion related to the loss of material from the wall surface, but they do not consider the moving boundary effects due to the material loss.
- The present analysis deals with pure erosion due to the hydrodynamic interactions of waste flow against the wall boundary. Chemical corrosion was not considered.
- The slurry flow regime is assumed to be fully turbulent, and particles are homogeneously distributed. Reynolds number is in the range of 10^5 based on the tank diameter and operating conditions. The average flow velocity of fluid-solid flow is much larger than the critical entrainment velocity of solid particles.
- Waste slurry fluid is assumed to exhibit Newtonian behavior.
- The solid particle collisions are assumed to be elastic in the sense that no kinetic energy is dissipated as a result of the collision against the wall surface. This is realized through a coefficient of restitution, which is the ratio of the approach to recoil velocities and is specified as an input parameter to the code. This assumption is acceptable because only the wall shear driver for erosion is being calculated, not the actual removal of wall material.
- The particle shape contained in the waste flow is assumed to be spherical. The particle size is

uniform and about 100 microns in diameter on the average.

From a nodalization study, an optimum number of about 200,000 nodes was established for the final analysis of the three-dimensional erosion model. The optimum number was determined by the criterion that the numerical results are independent of mesh sizes within about 0.1 % uncertainty. A finer non-uniform grid was used in the corner zones and joint sections where potential flow direction changes and flow splits might occur. Very fine meshes, less than 0.05 in long, were used near the misalignment and connection joints to capture the high velocity gradients.

Based on the modeling assumptions, the continuous and discrete phase equations were coupled to compute the particle trajectories and find the locations of high wall shear where the highest erosion is assumed to occur. In the analysis, flow patterns, wall shear, and vorticity distributions were considered as the key parameters for capturing flow characteristics and providing information on potential damage sites caused by abrasive erosion. All converged solutions were achieved using the segregated and iterative solution technique.

BENCHMARKING RESULTS

From the literature information, the principal drivers for erosion for a solids laden fluid were identified. These were the solids content of the working fluid, the regions of recirculation and particle impact with the component walls, and the regions of high wall shear. The CFD models for wall shear and particle impingement erosion were developed using Fluent^{TM} [4] and calculations were performed to estimate slurry-flow patterns, wall shear, and particle paths in components and fittings representative of those in the SME and MFT.

The model predictions were benchmarked against the literature data for hydraulic transport and erosion tests. Three sets of representative experiments were chosen to test the CFD models presented in this paper. They are the hydraulic tests obtained for sharp-edged (so-called miter) and 90° standard elbows [5], and erosion test data for the straight pipe [6]. All these tests were performed using a sand-water slurry. For the hydraulic experiments through the elbows, a 30.2-mm pipe diameter and about 990-micron particles were used. Solid concentrations for the sharp-edged and standard elbows were 8 and 20 weight percent, respectively. The results of the model predictions are compared with the test data in Fig. 3, and agree with the experimental data to within about 15%.

For the erosion experiment, Hisamitsu et al. [6] used a straight pipe with an inside diameter of 75 mm through which the slurry flowed at 2.83 m/s. The slurry had a nearly-uniform size distribution of sand of an approximate diameter of 0.67 mm with a specific gravity of 2.7 and a concentration of solids of 11 vol.%. Erosion was measured at 8 points along the pipe circumference with an ultrasonic thickness meter. Using the parameters from this straight pipe experiment, predictions were made with the particle impingement model. Those predictions are compared with the test data in Fig. 4. The results show that the model predictions qualitatively similar to the data. The locations of high and low erosion sites are in close agreement, while the relative difference between the maximum and minimum erosion rate based on the particle impingement rate agrees with the data to within about 20%. This results in a validation of those calculations, and will allow the test results to be applied to a prediction of erosion in the facility in those regions where the phenomenological drivers are expected to be similar.

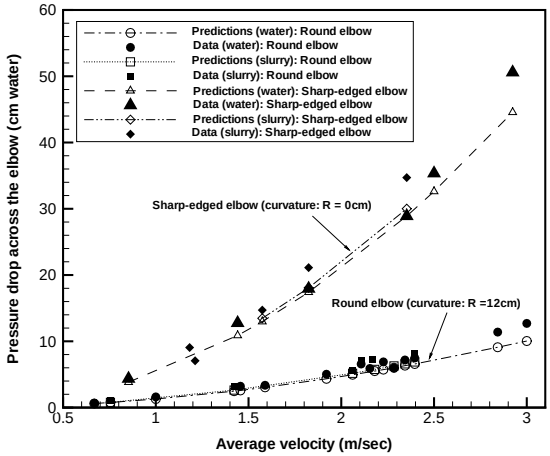

Figure 3. Comparison of predictions using the standard κ–ε turbulent model with discrete solid phase to the experimental hydraulic data of Masayuki et al. [5]

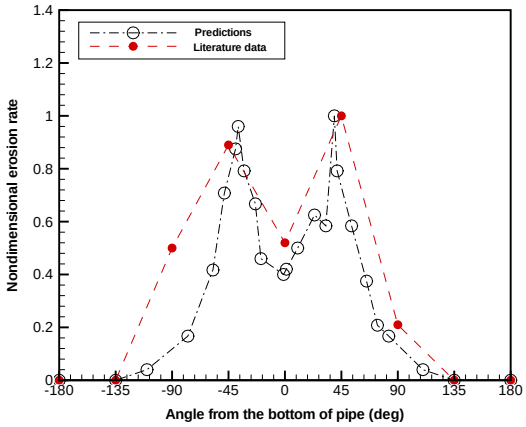

Figure 4. Comparison of predictions, using the standard κ–ε turbulent model with discrete solid phase, to experimental erosion data for horizontal pipe of Hisamitsu et al. [6] (Pipe diameter = 75 mm, average slurry velocity = 2.83 m/sec, solid vol. conc. = 11%, particle size = 0.67 mm).

MODELING RESULTS AND DISCUSSIONS FOR SLURRY MIXER TANK

An evaluation of the erosion drivers for two different coil guide geometries was performed to observe the erosion damage patterns for the areas near the coil guides as shown in Fig. 2, as well as to examine the sensitivity of the flow and erosion patterns to the disappearance of the coil guide lead-in plate. These modeling objectives for the two cases

are summarized in Table 2. Table 1 shows typical conditions for key operating parameters of the SME and MFT tanks. The results were used to identify the potential locations of high erosion for the SME coil guide and its support structure and in estimating the maximum allowable speed of the MFT agitator.

The results of wall shear distributions for Case-A are compared for two different velocities with a 60^o flow incidence into the coil guide region. The results show that the locations of high erosion sites are not changed when the velocity is increased. The high erosion sites are not sensitive to the variations of incident angles, but the 30^o incident flow field creates an overall erosion patterns closer to the one observed in the tank inspections. When the incidence angle of flow is changed from 60^o to 30^o, wall shears on the front lead-in plate and the tank floor regions in front of the lead-in plate and below the coil support are increased (higher shear areas in the upstream region in Fig. 5) because of the increased contribution at the boundary from the radial flow component in the global calculation. The results are compared under the original configurations of the coil guide shown in Fig. 5. The calculated locations of the high erosion sites are consistent with the ones observed in the recent inspections [7] as shown in the figure.

The pattern of high particle impingement regions is qualitatively different from the observed wear patterns in the SME. However, the flow pattern results show that the region near the tank floor area between the lead-in plates has the highest flow corresponding to one of the high erosion sites as observed by the recent inspections [7]. A series of calculated results shows that the loss of the leading edge of the coil guide due to the erosion damage does not affect the erosion patterns, and that the radial flow contribution to the location of erosion site is insignificant. Some comparisons of these patterns are shown in Fig. 6.

The sites of high abrasive erosion and the degree of erosion-driven damage due to the wall shear mechanism for the three typical flow conditions shown in Table 1 are compared in Fig.7. The results presented in the figure are compared under the same color scale in Fig. 8. It is clearly indicated that the calculated wall shear patterns agree with observed wear patterns. Quantitative results for three high erosion sites are compared for three different speeds of the tank agitator in Table 3. The results show that when the MFT agitator operates between 65 rpm and 103 rpm, the leading edge of the coil guide will be damaged by the abrasive wall erosion, but maximum wall shear for the MFT tank floor below the coil tab is about 87 Pa, which is well below the value of about 169 Pa that led to the serious erosion of the coil guide lead-in as observed in the SME inspections.

Measurements of erosion in the SME showed the upstream coil lead-in completely removed, tank floor erosion in Region 1 of about 3/8-in, and floor erosion in Region 2 of about 1/16 – 1/8-in. The wall shear stresses shown in Table 3 indicate that the maximum shear stress expected in the MFT (103 rpm) in Region 1 is slightly less than that observed in Region 2 of the SME calculation (130 rpm). Therefore, while the coil guide lead-in might be eroded in the MFT, the tank floor would not be eroded any more than the degree observed in Region 2 of the SME, viz., no more than 1/8-in. A linear extrapolation of the data based on wall shear stress would indicate an erosion of about 0.05 in in the MFT in Region 1 and none in Region 2. Table 3 also indicates that virtually no erosion from wall abrasion would be expected for impeller speeds of 65 rpm. The results demonstrated that the predicted wall shear patterns compare well with observed sites of high erosion as well as relative magnitude of erosion depth.

An additional calculation was performed to understand the behavior of the eroded cavities on the tank floor. The nominal model was extended to evaluate different cavity sizes and gap distances at the three different speeds because of the tilted tank floor. The cavity was modeled by locating a half-section ellipsoid 2.3 in wide and 0.35 in deep (or 2.8 in wide and 0.6 in deep for the larger cavity) on the tank bottom near the coil restraint as shown in Fig. 2. The results were evaluated by comparing the magnitude of the calculated wall shear in the cavities to that which led to the measured erosion depths at the various sites on the tank floor. The results showed that serious erosion can occur to the tank bottom downstream of the cavity region when the agitator impeller operates continuously at 130 rpm. The shear stress on the bottom surface of the cavity was low in all cases, indicating that the rate at which cavity depths grows slows and likely stops when the cavity becomes sufficiently deep. When the cavity size increases, separation of boundary layer on the cavity surface occurs with secondary flow generated as shown in Fig. 9. The shear stresses associated with the recirculating flow are much lower as shown in Table 4. The mechanism for boundary layer separation and the variables that affect it have not been addressed here, but they are the subject of ongoing work to be reported by the authors at a later date.

SUMMARY AND CONCLUSIONS

This paper presents the application of computational fluid dynamics (CFD) methods to a qualitative estimate of the erosion phenomena expected in the SME and MFT process tanks. The modeling results show that primary locations of the highest erosion due to the abrasive wall erosion are at the leading edge of the guide, the tank floor below the insert plate of the coil guide, and the upstream side plate of the top lead-in plate. The predicted erosion sites are in good agreement with the visual observations done by the recent SME inspections [7].

A series of the modeling results indicates that potential high erosion sites for the current geometry of the coil guide are related primarily to the abrasive wall shear rather than particle impingement since the predicted shear patterns agrees well with the degree of erosion. The relative magnitude of shear stress also compares well with depth of erosion. It is noted that the loss of the leading edge of the coil guide due to the erosion damage during the SME mixing

operation does not affect the erosion patterns on the tank bottom. Results of cavity sensitivity to erosion depth indicate that the magnitude of wall shear in the bottom of cavity decreases and continued erosion ceases because of boundary layer separation when the cavity becomes sufficiently large.

REFERENCES

1. Tiberia, S. L., C.T, Chandler, C.F. Jenkins, S.Y. Lee, A. P. Rangus, S.L.West, 2003, Independent Review of the Slurry Mix Evaporator Repairs, Washington Savannah River Company, CBU-WSE-2003-0050.
2. Lee, S. Y., and Dimenna, R. A., 2002, "Erosion Analysis for the Misaligned U2 Nozzle and Its Connector Block", Washington Savannah River Company, WSRC-TR-2002-00352, April.
3. Lee, S. Y., Dimenna, R. A., and Duignan, M. R., 2002, "Designing a Scaled Erosion Test with Computational Fluid Dynamics Methods", Proceedings of FEDSM2002: 2002 ASME Fluids Engineering Division Summer Meeting, Paper No. FEDSM2002-31285, Montreal, Quebec, Canada, July 14-18.
4. FLUENT, 1998, Fluent, Inc., Lebanon, New Hampshire.
5. Masayuki, T., Norio, K., Shozaburo, S., and Siro, M., 1972, "Hydraulic Conveying of Solids thruough Pipe Bends", J. of Chemical Engineering of Japan, vol. 5, No. 1, pp. 4-13.
6. Hisamitsu, N., Iseh, T., and Takeishi, Y., 1981, "An experimental study on pipe erosion by sand slurry", Proc. 6th Conference on Slurry Transportation, Slurry Transport Association, pp. 319-332.
7. Hinz, W. R., 2003, Nondestructive Examination Condition Report, Savannah River National Laboratory, SRT-MTS-2003-60109, February 13, 2003.

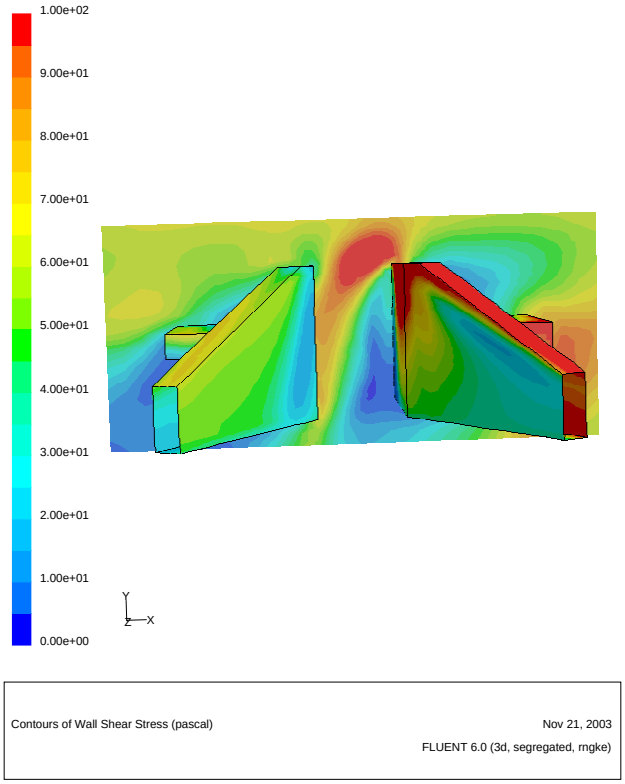

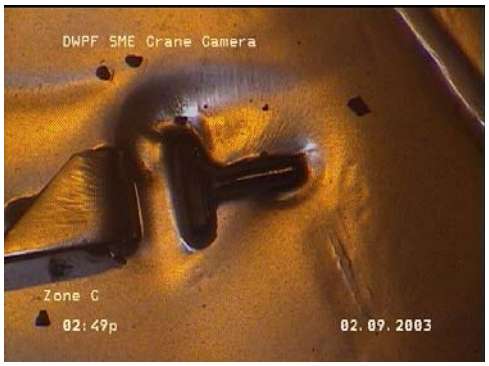

Figure 5. Comparison of the predicted high wall shear indicated on the right lead-in plate (left) to the worn-away lead-in plate shown in the visual inspection photo (left) (the model predictions based on 130 rpm (1.8 m/sec) and 30^{o} flow incidence)

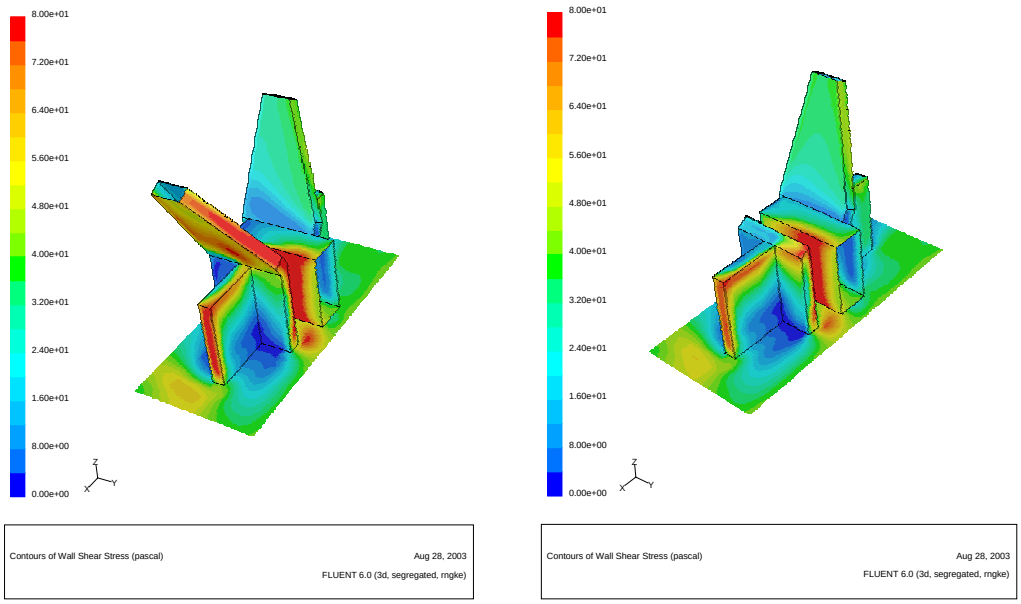

Figure 6. Comparison of wall shears between two cases for 103 rpm with 30^{o} incidence angle of slurry flow into the guide pin

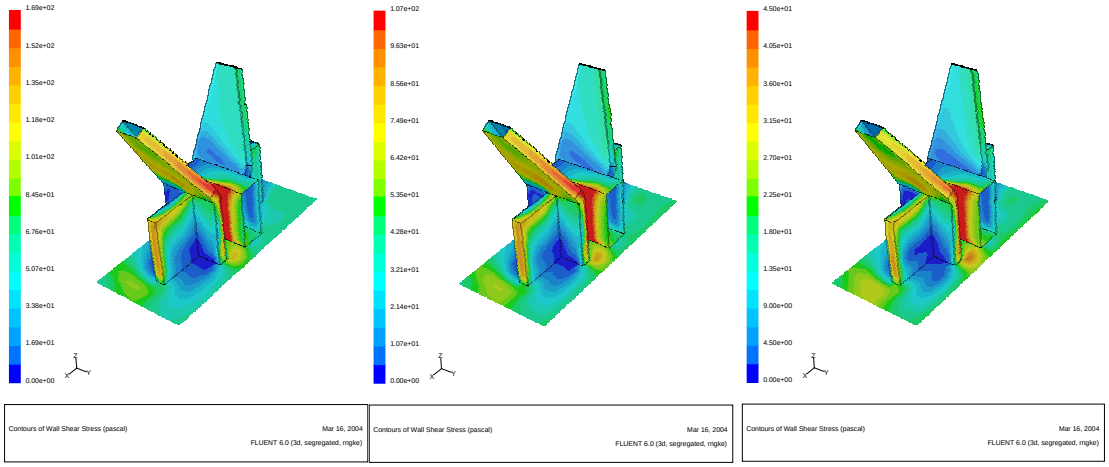

(130 rpm) (103 rpm) (65 rpm)

Figure 7. Comparison of abrasive wall shear patterns between three different cases with 30^{o} incidence angle of slurry flow into the guide pin

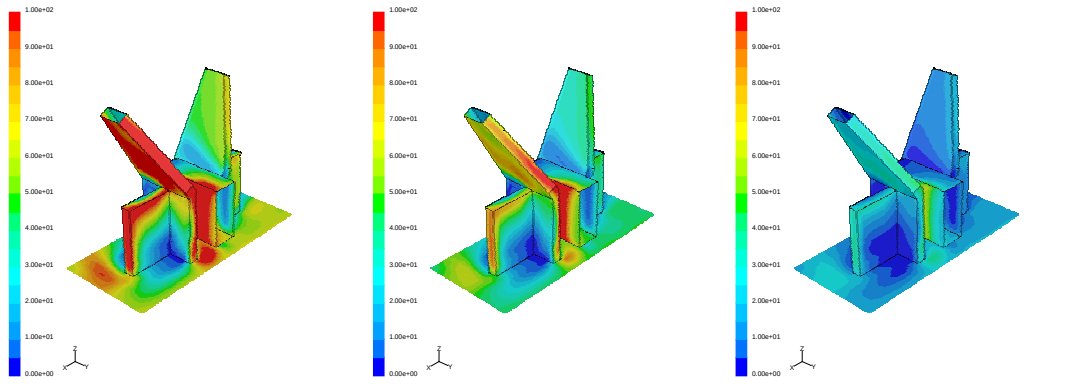

Figure 8. Comparison of abrasive wall shears between three different cases with 30^{o} incidence angle of slurry flow into the guide pin under the same color scale

Table 3. Maximum wall shears for key erosion areas

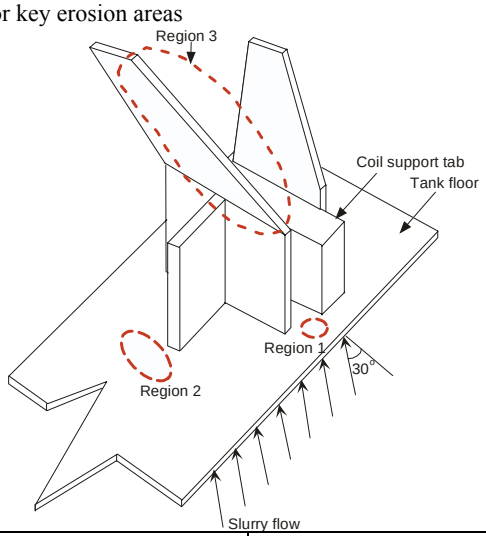

Slurry velocity (agitator speed)	Region 1 (Process vessel)		Region 2 (Process vessel)		Region 3 (Process vessel)	
	(MFT)	(SME)	(MFT)	(SME)	(SME)	(MFT)
0.65 m/sec (65 rpm)	39 Pa	39 Pa	29 Pa	29 Pa	41 Pa	41 Pa
1.3 m/sec (103 rpm)	87 Pa	--	65 Pa	--	107 Pa	--
1.8 m/sec (130 rpm)	N/A	127 Pa	N/A	96 Pa	N/A	169 Pa
Measured erosion depth	No data	.35 in	No data	.094 in	No data	> 0.5 in

Table 4. Maximum wall shears at the bottoms of two different cavity sizes on the SME tank floor and two different gap sizes for 130 rpm operating conditions

Gap size between the lower end of coil support tab and tank floor	1 in gap		0.5 in gap	
Cavity depth on tank floor	0.35 in	0.6 in*	0.35 in	0.6 in*
Max. wall shear at cavity bottom	56 Pa	55 Pa	59 Pa	57 Pa

Note:*This size was used only for sensitivity calculations, but it has not been observed by the visual inspection.

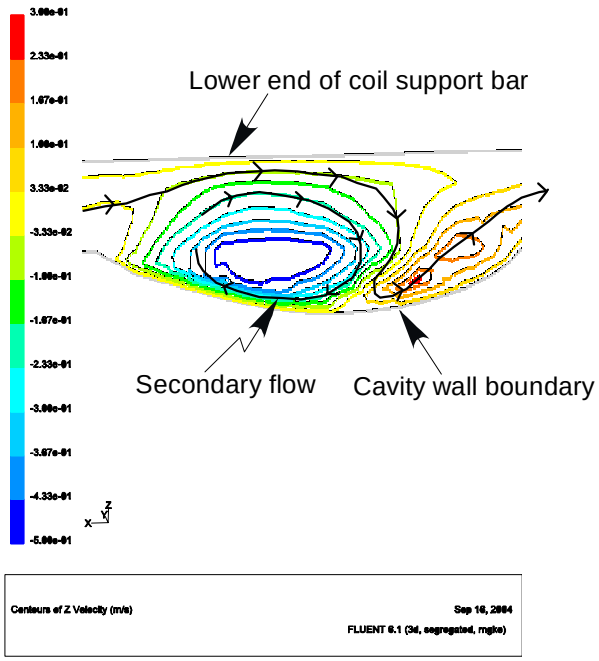

Figure 9. Velocity contour plot for the gap region between 0.35 in deep cavity wall and the lower end of coil support